Electronic Supplementary Material (ESI) for RSC Advances.

Construction of the ternary hybrid of CdS Nanoparticles Loaded on Mesoporous TiO_2/RGO for Enhancement of Photocatalytic Activity

Hongwei Tian[a*], Chenxing Wan[a], Weitao Zheng[a, b*], Xiaoying Hu[c], Liang Qiao[c], Xiaoyi Wang[d],

[a] Department of Materials Science and Key Laboratory of Automobile Materials of MOE, Jilin University, Changchun, China.

[b] State Key Laboratory of Automotive Simulation and Control, Jilin University, Changchun, China.

[c] College of Science, Changchun University, Changchun, China

[d] Key Laboratory of Optical System Advanced Manufacturing Technology, Changchun Institute of Optics, Fine Mechanics and Physics, Chinese Academy of Sciences, Changchun, 130033, China

Corresponding authors:

[*]E-mail: tianhw@jlu.edu.cn, wtzheng@jlu.edu.cn.

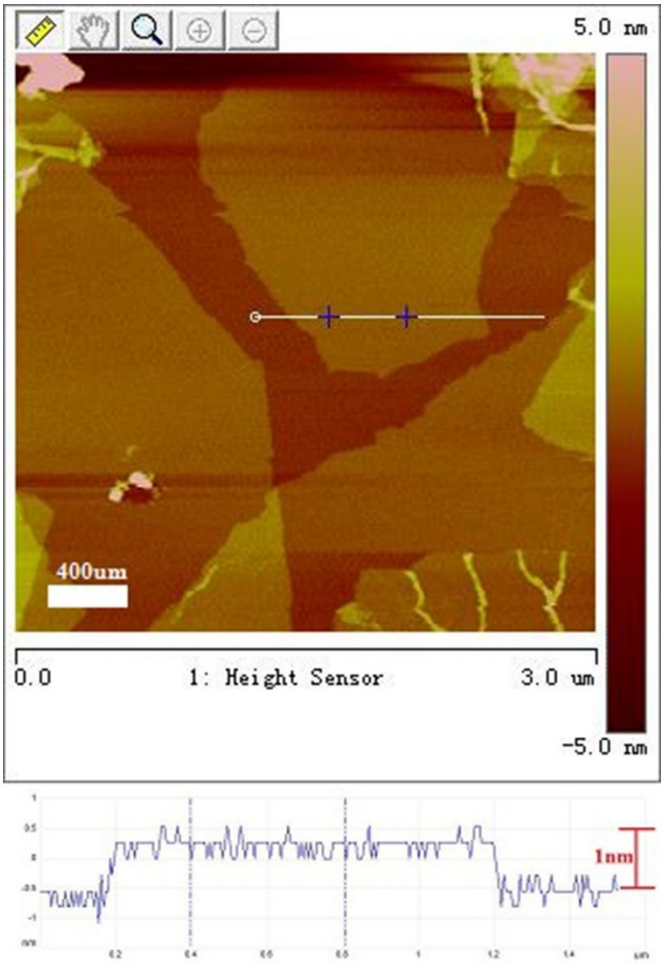

Fig. S1. Atomic Force Microscope (AFM) image of graphene oxide (GO) after ultrasonic.

Fig. S1 shows the typical AFM image and the corresponding cross-sectional view of GO. It is observed that the mica substrate is covered with a number of nanosheets with different size. It is obviously that the average thickness of GO nanosheets is about 1 nm.

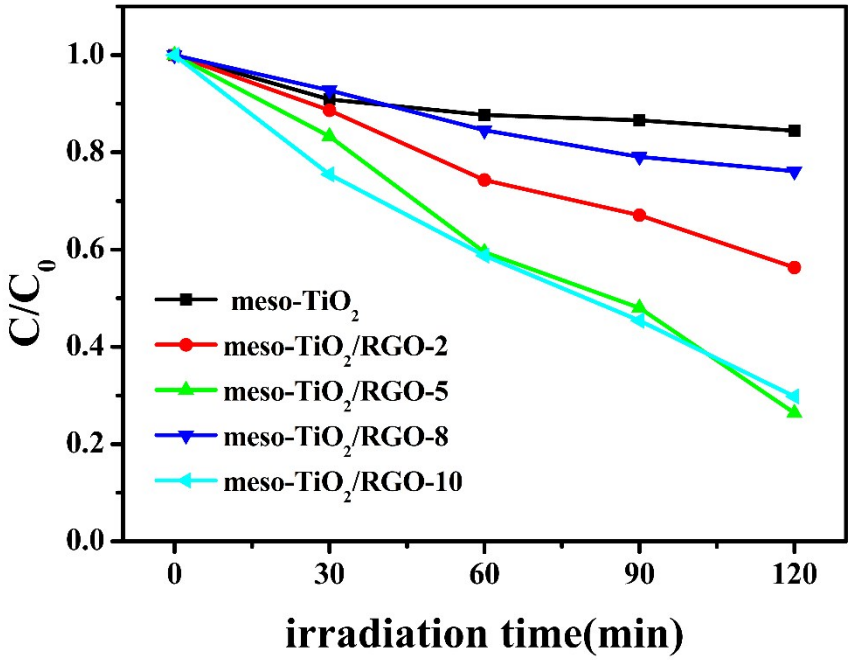

Fig. S2. Photodegradation of the MO for meso-TiO_2/RGO-x (x=0, 2, 5, 8, 10. x on behalf of the mass fraction of RGO) under the irradiation of the simulated solar light.

The photodegradation to MO of binary meso-TiO_2/RGO-X composites as shown in Fig. S2. The degradation ability varies with the different mass fraction of RGO. Among them, the photodegradation activity of meso-TiO_2/RGO-5 is greatest. Therefore, choosing meso-TiO_2/RGO-5 as the best sample fulfills the compound of the third components.

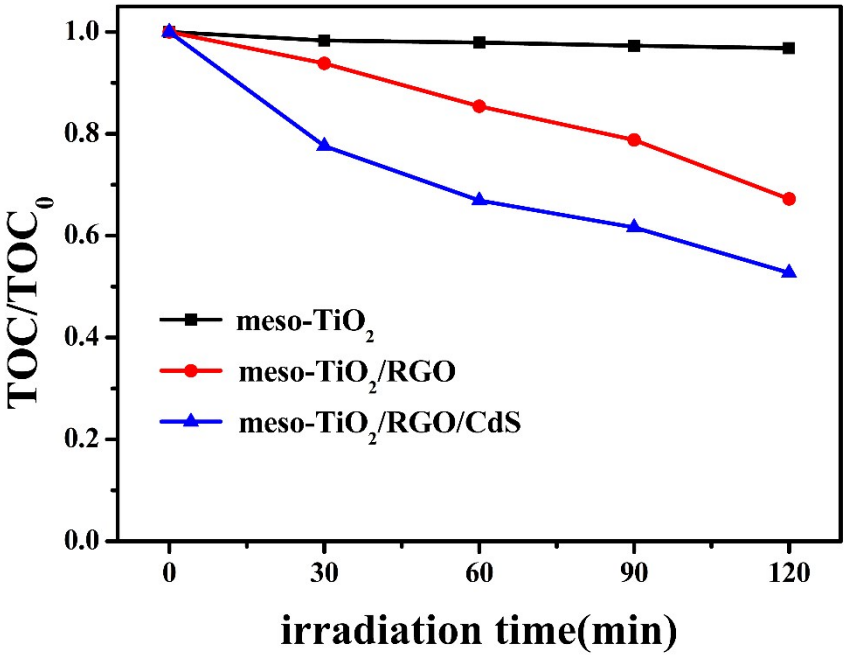

Fig. S3.TOC removal of the MO for meso-TiO_2, meso-TiO_2/RGO, meso-TiO_2/RGO/CdS.

Reaction conditions: MO concentration, 10mg/L; the mass of catalyst, 20mg; under the irradiation of the simulated solar light.

The photocatalytic performance of meso-TiO_2, meso-TiO_2/RGO and meso-TiO_2/RGO/CdS in aqueous contaminant can also be evaluated by TOC removal. The change of TOC concentration reflected the mineralization degree of MO dye in Fig. S3. The TOC removal contents of meso-TiO_2, meso-TiO_2/RGO and meso-TiO_2/RGO/CdS respectively are 3.4%, 32.8%, 47.1% under the simulated solar light irradiation for 120 min. The ternary meso-TiO_2/RGO/CdS catalyst shows the highest TOC removal rate of MO among the tested samples, which bascially coincides with the result of the degradation rate. This phenomenon suggests that MO molecules are most likely mineralized into inorganic molecules.

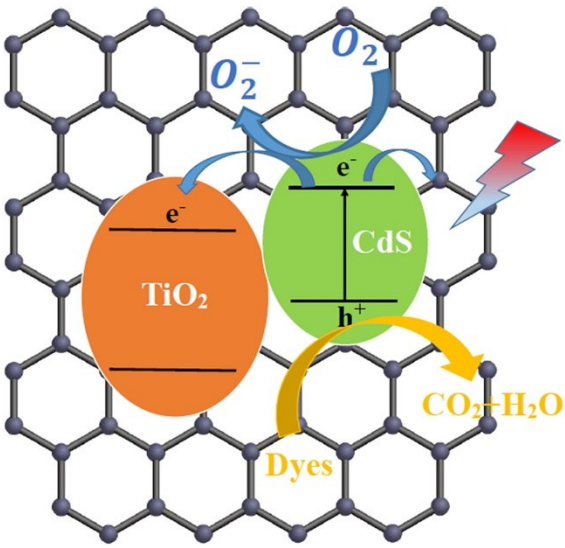

Fig. S4. Proposed mechanism diagram illustrating the photocatalytic redox reactions with the ternary meso-TiO_2/RGO/CdS catalyst under visible light.

Fig. S4 signifies CdS plays the major role in which the electrons are excited from the VB to the CB and the hole left in VB. The electrons besides dissolving oxygen molecule and transferring to graphene nanosheets can also transfer to the CB of TiO_2. Meanwhile, because the E_{VB} of CdS (+1.88V vs. NHE) is not more positive than the standard redox potential of •OH/H_2O (2.38 V vs. NHE), so the holes of CdS can not react with H_2O and –OH. But the holes themselves have the strong oxidation ability and can directly oxidize dyes into CO_2 and H_2O.